

Investigation of the structure of many-particle exciton-impurity complexes bound to phosphorus atoms in silicon

A. S. Kaminskiĭ, V. A. Karasyuk, and Ya. E. Pokrovskii

Institute of Radio Engineering and Electronics, Academy of Sciences of the USSR, Moscow

(Submitted 7 June 1982)

Zh. Eksp. Teor. Fiz. 83, 2237-2251 (December 1982)

The fine structure of no-phonon luminescence lines α_m (m is the number of bound excitons) due to many-particle exciton-impurity complexes bound to phosphorus atoms in silicon was investigated experimentally and theoretically. The fine structure was calculated for an excited state of a bound exciton ignoring the interaction with an inner-shell electron Γ_1 , even in the presence of uniaxial strains and magnetic fields. One-particle wave functions were used in this calculation and an allowance was made for the symmetry of the electron and hole states dependent on the direction and sign of strain. In these approximations the fine structure was found to be governed by six interaction constants. On compression along the [001] axis the spectrum of the α_2 line consisted of three components, but four components were observed when tension was applied. A comparison of the calculations and experiments yielded the interaction constants, which were then used to calculate other spectra. The calculated spectra of the α_2 line in magnetic fields were in good agreement with the Zeeman α_2 spectra recorded on compression along the [001] axis. An investigation was made of the spectra of the α_2 line in the case when strains were applied along the [111] and [110] axes. A numerical calculation was made of these spectra and a qualitative agreement with the experiments was obtained. In the absence of strain, about ten components were resolved in the α_2 spectrum. Energy level schemes were proposed for the initial and final states and these accounted for the structure of the α_2 line. Details of the fine structure of the α_3 and α_4 lines could not be resolved, probably due to the large number and broadening of the components.

PACS numbers: 71.35. + z, 71.55.Dp, 71.70.Ej

1. INTRODUCTION

Many-particle exciton-impurity complexes (MEICs) are formed as a result of capture of m excitons by a neutral donor or acceptor in a semiconductor¹ and they consist of a singly charged impurity ion and $2m + 1$ electrons and holes. A shell model^{2,3} of MEICs accounted for the main features of the recombination radiation spectra observed on dissociation of these complexes and for changes in the spectra due to strain and magnetic fields (for reviews see Refs. 4 and 5). According to the shell model, in the case of MEICs bound to group V donors in silicon, there are two electrons at the lower energy level of symmetry Γ_1 , whereas the other $m - 1$ electrons are distributed between triply and doubly degenerate shells Γ_5 and Γ_3 , split off by the interaction with the donor field. The ground state of holes is a quadruply degenerate shell Γ_8 . When electrons from the Γ_1 shell recombine, they give rise to luminescence lines designated by α_m . Since the wave functions of electrons in the Γ_1 state do not have a node in a cell occupied by a donor, such recombination may result in the transfer of quasimomentum to the impurity ion of a complex and the α_m lines are then observed not only in the phonon (TA, LO, and TO) but also in the no-phonon (NP) parts of the spectra.

Uniaxial deformation of silicon along the [001] axis results^{5,6} in splitting of the Γ_8 hole state and of the Γ_5 and Γ_3 electron states, and it causes a nonlinear shift of the Γ_1 state.

Figure 1 shows the dependences of the spectral positions of the α_1 lines on the pressure P applied along the [001] axis in silicon doped with phosphorus and arsenic. It is clear

from this figure that the dependence for the α_1 line is sublinear at low pressures. This sublinear shift indicates inequivalence of the electron orbitals in an MEIC in the Γ_1 state. In fact, a uniaxial compression of a neutral donor along the [001] axis results in mixing of the Γ_1 and Γ_3 states, so that the energy of the Γ_1 state increases and in the high-compression limit it rises by $2\Delta_2^0/3$, where Δ_2^0 is the splitting between the Γ_1 and Γ_3 states in the absence of strain.⁷ A similar shift of the Γ_1 level should also occur in a bound exciton, because in this case the shift obtained in the strong-compression limit is again $2\Delta_2^0/3$, where Δ_2^0 is the Γ_1 - Γ_3 splitting exhibited by a bound exciton when the pressure is $P = 0$. It follows that the

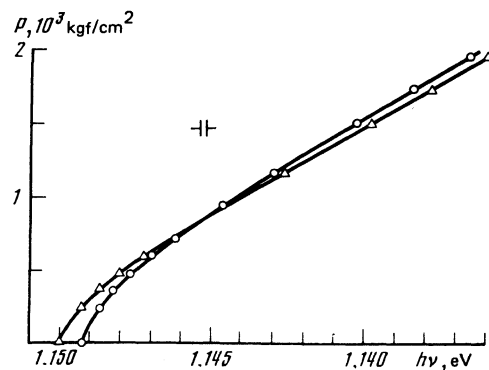


FIG. 1. Dependences of the spectral positions of the luminescence line of excitons bound to phosphorus (Δ) and arsenic (\circ) atoms in silicon on the pressure P applied along the [001] axis at 4.2 °K.

energy of the final state of a neutral donor increases by $2\Delta_2^0/3$, whereas the energy of the initial state on equivalent electron orbitals in a bound exciton should rise by $2 \times 2\Delta_2^1/3$. It therefore follows that the difference between the energies of the initial and final states for the α_1 line should change as a result of compression by $4\Delta_2^1/3 - 2\Delta_2^0/3$. According to Refs. 8 and 9, in the case of phosphorus we have $\Delta_2^0 = 13$ meV, $\Delta_2^1 = 4.2$ meV, whereas in the case of arsenic we have $\Delta_2^0 = 22.5$ meV, $\Delta_2^1 = 5.8$ meV. This should cause an additional splitting of the α_1 lines toward lower energies (compared with the linear shift caused by a reduction in the band gap), which amounts to ≈ 3 meV in the case of phosphorus and ≈ 7 meV in the case of arsenic, i.e., it should give rise to a superlinear dependence of the shift of the α_1 line on P in the direction of the red part of the spectrum.

This conflict between the predictions and experiment can be removed if we assume that the Γ_1 state corresponds to electron orbitals with very different localizations. Although this goes beyond the shell model, it seems a natural assumption. In fact, a theoretical analysis of a D^{-1} center in a many-valley semiconductor,¹⁰ when such a center consists of a positively charged ion and two electrons, gives results which are in agreement with experiment only if we select electron orbitals differing by a factor of approximately 3.5 in respect of the localization parameters. If we assume, as in the case of the D^{-} centers, that one of the orbitals of a bound exciton is analogous to an orbital of a neutral donor, a strong compression along the [001] axis should increase the energy of the initial state by $2\Delta_2^0/3 + 2\Delta_2^1/3$ and give rise to an additional (compared with the linear) shift of the α_1 line toward higher energies by about $2\Delta_2^1/3$, i.e., by 2.8 meV in the case of phosphorus and by 4 meV in the case of arsenic. We can see quite clearly from Fig. 1 that this blue shift of the α_1 line is stronger in the case of arsenic.

It follows that the electron state Γ_1 in an MEIC in a ground or excited state is analogous to an electron state of D^{-} and D^0 , respectively. Therefore, from now on we shall assume that the interaction of electrons and holes in an MEIC with electrons in the Γ_1 state does not result in a significant splitting of the energy levels of the complexes bound to donors in silicon. In fact, in the initial state the Γ_1 -shell electrons form a spin singlet and do not contribute to the exchange interaction. In the final (excited) state created as a result of a transition α_m , only one unpaired electron remains in the Γ_1 shell and the wave function of this electron is analogous to the wave function of an electron at a neutral donor, i.e., this wave function is strongly localized near the impurity ion. Consequently, the exchange interaction of this electron with other electrons and holes is slight. It follows that in calculating the splitting of the energy levels of an MEIC, which is responsible for the fine structure of the α_m lines,^{11,12} we should allow only for the interaction between holes themselves, and also between holes and electrons in the outer shells. We shall use the results of such a calculation in a quantitative interpretation of the NP fine structure of the α_m lines which are observed on dissociation of P_m complexes bound to phosphorus atoms in silicon, including those ob-

served under uniaxial compressive and tensile stresses and in magnetic fields. In our study the spectral resolution was improved by employing an interference method described in Ref. 13. Other details of the experiments will be given in the presentation of the results.

2. INTERACTION OF AN ELECTRON IN A $\Gamma_5 \times \Gamma_6$ STATE WITH A HOLE IN A Γ_8 STATE, BOTH BOUND TO AN IMPURITY CENTER IN SILICON

We shall now consider changes in the energy spectrum caused by the interaction between an electron and a hole bound to an impurity center in the case when the wave functions of the electron and hole transform respectively in accordance with the $\Gamma_5 \times \Gamma_6$ and Γ_8 representations of the T_d group. This interaction should determine the fine structure in the spectrum of an excited state of a bound exciton P_1^* , which is the final state of a transition α_2 , because—according to our model—we can ignore the interaction with an electron in the Γ_1 state.

The number and symmetry of the wave functions are governed by the symmetry of the initial one-particle states and are found by expanding, in terms of irreducible representations, the direct product of the representations used to transform the one-particle wave functions of an electron and a hole. In this case the interaction of an electron and a hole causes splitting of a term into ten levels, whose number and symmetry are given by the expansion

$$D = \Gamma_5 \times \Gamma_8 \times \Gamma_6 = 3\Gamma_4 + 3\Gamma_5 + 2\Gamma_3 + \Gamma_2 + \Gamma_1. \quad (1)$$

We shall use the method of invariants¹⁴ to construct the interaction Hamiltonian. We shall use the basis in the form of linearly independent matrices constructed from the momentum operator matrices L_i , J_i , and σ_i expressed in terms of the following bases:

$$\begin{aligned} & x, y, z; \\ Y_{3/2}^{3/2} &= -\frac{1}{\sqrt{2}}(X+iY)\alpha, \quad Y_{-3/2}^{3/2} = \hat{K}Y_{3/2}^{3/2}; \\ Y_{1/2}^{3/2} &= -\frac{1}{\sqrt{6}}[(X+iY)\beta - 2Z\alpha], \quad Y_{-1/2}^{3/2} = \hat{K}Y_{1/2}^{3/2}; \\ & \alpha, \beta. \end{aligned} \quad (2)$$

Here x, y, z and X, Y, Z are, respectively, the coordinate parts of the electron and hole functions in the states Γ_5 and Γ_8 ; α and β spinors; \hat{K} is the time reversal operator.

It follows from Ref. 14 that the matrix of the interaction of an electron with a hole \mathcal{H}^{eh} can be represented as a linear combination of direct products of the matrices constructed from the matrices L_i , J_i , and σ_i invariant under the T_d group transformations. The number of such independent invariants corresponds to the number of unit representations occurring in the expansion of the direct product $D \times D$ and it amounts to 24. An additional condition imposed on the matrix \mathcal{H}^{eh} is the invariance under time reversal, and in this case the number of invariants decreases to 17. These invariants were constructed using a method developed in Ref. 7. However, we also assumed that "intervalley" matrix elements containing wave functions of electrons from different valleys are small and can be ignored. This reduced the number of invariants to seven so that the Hamiltonian of the

interaction between an electron and a hole could be represented in the form

$$\begin{aligned} \mathcal{H}^{eh} = & \Delta_0 I + \Delta_1 I_L \times \left(\sum_i J_i \times \sigma_i \right) + \Delta_2 I_L \times \left(\sum_i J_i^3 \times \sigma_i \right) \\ & + \Delta_3 \sum_i (L_i^2 - 2/3 I_L) \times J_i \times \sigma_i + \Delta_4 \sum_i (L_i^2 - 2/3 I_L) \times J_i^3 \times \sigma_i \\ & + \Delta_5 \sum_{i,j,h} \varepsilon_{ijk} L_j^2 \times V_h \times \sigma_h + \Delta_6 \sum_i (L_i^2 - 2/3 I_L) \times J_i^2 \times I_\sigma; \\ V_i = & \sum_{j,h} \varepsilon_{ijk} [J_i, J_j^2], \quad [J_i, J_j] \equiv 1/2 (J_i J_j + J_j J_i). \end{aligned} \quad (3)$$

Here ε_{ijk} is an antisymmetric unit pseudotensor, whereas I_σ and I_L are two and three-dimensional unit matrices which we shall subsequently omit. The interaction constants Δ_i determine the contributions of the corresponding invariants to the electron-hole interaction and can be found from the experimental results. The terms occurring in Eq. (3) can be interpreted as follows. The parameter Δ_1 gives the value of the isotropic part of the electron-hole exchange interaction, Δ_2 gives the anisotropy of the exchange interaction resulting from the nonsphericity of the hole wave function, whereas Δ_3 , Δ_4 , and Δ_5 represent the exchange isotropy associated with the anisotropy of the electron wave function, and Δ_6 is the crystal splitting contribution.

In a magnetic field \mathbf{H} and under a strain ε we must supplement Eq. (2) by the matrices $\mathcal{H}(\mathbf{H})$ and $\mathcal{H}(\varepsilon)$ describing the interaction of an electron and a hole with the magnetic and strain fields, respectively. The matrix of the interaction with the strain field is

$$\begin{aligned} \mathcal{H}(\varepsilon) = & E_{1g} \sum_i \varepsilon_{ii} + b' \sum_i \left(J_i^2 - \frac{5}{4} \right) \varepsilon_{ii} \\ & + \frac{2d'}{\sqrt{3}} \sum_{i<j} [J_i, J_j] \varepsilon_{ij} - \Xi_u \sum_i \left(L_i^2 - \frac{2}{3} \right) \varepsilon_{ii}. \end{aligned} \quad (4)$$

Here $E_{1g} = (\Xi_d + 1/3 \Xi_u - a)$; b' , d' , Ξ_d , and Ξ_u are the deformation potential constants of a hole and an electron bound to an impurity center; ε_{ij} is the strain tensor. The interaction with the magnetic field is described by the matrix

$$\mathcal{H}(\mathbf{H}) = \mu_0 g_i^h \sum_i J_i H_i + \mu_0 g_e^h \sum_i J_i^3 H_i + 1/2 \mu_0 g^e \sum_i \sigma_i H_i. \quad (5)$$

Here, μ_0 is the Bohr magneton; g_i^h , g_e^h , and g^e are the g factors of a hole and an electron, H_i are the components of the magnetic field vector.

We shall conclude this section by noting that the expressions (2)–(5) are valid if the characteristic energies of the electron-hole interaction are small compared with the binding energy of carriers to a center.

3. FINE STRUCTURE OF THE α_2 LINE IN THE CASE OF UNIAXIAL DEFORMATION OF SILICON IN THE [001] DIRECTION

Uniaxial deformation of silicon crystals results in partial lifting of the degeneracy of electron and hole states in an MEIC. A quadruply degenerate hole state Γ_8 splits into two doubly degenerate states. The lowest hole state of an MEIC

bound to a donor is already filled when the number of excitons is $m = 2$. It should be pointed out that in the case of strong deformations (large strains), when the splitting of the hole state exceeds the binding energy of an MEIC attached to a donor, the complexes containing more than two holes are unstable.¹⁵ For $m = 2$ an MEIC contains two electrons and two holes, which form spin singlets, and also one unpaired electron. Therefore, the initial state for a α_2 transition in a uniaxially deformed silicon crystal is the singlet (in the absence of a magnetic field) state P_2 , whereas the final state is P_1^* , containing one hole, one electron in the Γ_1 state, and one electron in the excited state. Since in the adopted approximation the interaction with the Γ_1 electron is ignored, the fine structure of the α_2 line is governed by the interaction of the hole with the excited electron. The structure of the spectrum and its interpretation then simplify greatly. A similar simplification in the interpretation of the spectra is possible only under the action of a sufficiently strong magnetic field, when only the lowest spin sublevel is filled initially.

The simplest situation is obtained when silicon is strained along the [001] axis. In this case only ε_{xx} and ε_{zz} do not vanish, and the symmetry of an impurity center decreases to D_{2d} . The Γ_5 electron states splits into nondegenerate Γ_2 and doubly degenerate Γ_5 states, the hole level splits into Γ_6 and Γ_7 levels corresponding to the hole momentum $\pm 1/2$ and $\pm 3/2$. Under uniaxial compression the states with the lowest energy are Γ_2 and Γ_6 , the interaction between which determines the splitting of the final state P_1^* : $\Gamma_2 \times \Gamma_6 \times \Gamma_6 = \Gamma_3 + \Gamma_4 + \Gamma_5$, where Γ_3 and Γ_4 are nondegenerate and Γ_5 is doubly degenerate. The Hamiltonian of the interaction of an electron and a hole then contains three independent constants and if an allowance is made for the presence of a magnetic field, it can be written in the form

$$\begin{aligned} \mathcal{H} = & \bar{\Delta}_0 + \Delta_\perp (\sigma_x \times \sigma_x + \sigma_y \times \sigma_y) + \Delta_\parallel \sigma_z \times \sigma_z \\ & + \mu_0 (g_i^h + 5/2 g_e^h) (\sigma_x H_x + \sigma_y H_y) \\ & + 1/2 \mu_0 (g_i^h + 1/4 g_e^h) \sigma_z H_z + 1/2 \mu_0 g^e \sum_i \sigma_i H_i. \end{aligned} \quad (6)$$

The spectrum of the final state is found by solving the secular equation

$$|\mathcal{H} - \lambda I| = 0.$$

Comparing Eqs. (6) and (3) for the case of large pressures, we have

$$\begin{aligned} \bar{\Delta}_0 = & \Delta_0 + \Delta_6, \quad \Delta_\perp = \Delta_1 + 5/2 \Delta_2 + 1/3 \Delta_3 + 5/6 \Delta_4 - 3/4 \Delta_5, \\ \Delta_\parallel = & 1/2 \Delta_1 + 1/8 \Delta_2 - 1/3 \Delta_3 - 1/12 \Delta_4. \end{aligned} \quad (7)$$

If $H = 0$, the solution is

$$\lambda_{1,4} = \bar{\Delta}_0 + \Delta_\parallel, \quad \lambda_{2,3} = \bar{\Delta}_0 - \Delta_\parallel \pm 2 |\Delta_\perp|. \quad (8)$$

A magnetic field stops mixing of the states 2 and 3 of Eq. (8) (such mixing is due to the electron-hole interaction):

$$\begin{aligned} \lambda_{1,4} = & \bar{\Delta}_0 + \Delta_\parallel \pm 1/2 \mu_0 (g^e + g^h) H, \quad g^h = g_i^h + 1/4 g_e^h, \\ \lambda_{2,3} = & \bar{\Delta}_0 - \Delta_\parallel \pm [4 \Delta_\perp^2 + [1/2 \mu_0 (g^e - g^h) H]^2]^{1/4} \quad (H = H_z). \end{aligned} \quad (9)$$

When silicon is stretched along the [001] axis, the lowest electron state is the doubly degenerate Γ_5 state, whereas the lowest hole state is Γ_7 , corresponding to holes with the momentum $\pm 3/2$. In this case the interaction of an electron and a hole in the final state gives rise to a splitting $\Gamma_5 \times \Gamma_6 \times \Gamma_7 = \Gamma_1 + \Gamma_2 + \Gamma_3 + \Gamma_4 + 2\Gamma_5$ and the interaction Hamiltonian should generally have six constants. However, if—as before—we ignore the intervalley matrix elements, we find that the number of such constants decreases to four and the Hamiltonian becomes

$$\mathcal{H} = \Delta_0' + \Delta_{\perp}' (\sigma_x \times \sigma_x - \sigma_y \times \sigma_y) + \Delta_{\parallel}' \sigma_z \times \sigma_z + \Delta_T \sigma_z \times (\sigma_x \times \sigma_x + \sigma_y \times \sigma_y). \quad (10)$$

The secular equation gives the spectrum of the final state P_1^* :

$$\lambda_{1,4} = \Delta_0' + \Delta_{\parallel}' \pm 2|\Delta_{\perp}'|, \quad \lambda_{2,3} = \Delta_0' - \Delta_{\parallel}' \pm 2|\Delta_T|. \quad (11)$$

Comparing Eqs. (10) and (3), we obtain

$$\begin{aligned} \Delta_0' &= \Delta_0 + \frac{1}{2}\Delta_6, & \Delta_{\perp}' &= \frac{3}{4}\Delta_2 - \frac{1}{8}\Delta_4 - \frac{3}{8}\Delta_5, \\ \Delta_{\parallel}' &= \frac{3}{2}\Delta_1 + \frac{27}{8}\Delta_2 + \frac{1}{2}\Delta_3 + \frac{9}{8}\Delta_4, & \Delta_T &= -\frac{3}{8}\Delta_4 + \frac{3}{8}\Delta_5. \end{aligned} \quad (12)$$

It is clear from Eq. (1) that P_1^* splits into four levels under tension. If we ignore the anisotropy of the electron states, i.e., if we assume that $\Delta_3 = \Delta_4 = \Delta_5 = \Delta_6 = 0$, we find that the splitting is identical with that calculated in Refs. 16 and 17 for the interaction of a hole with a spherically symmetric electron state. It should be pointed out that the interaction with an electron in the Γ_1 state, which we regard as unimportant, is allowed for in the treatment given in Ref. 17.

We carried out an experimental study of the photoluminescence of silicon under uniaxial compression conditions paying special attention that the deformation should be homogeneous. As before,¹⁵ samples doped with phosphorus in a concentration of $2 \times 10^{14} \text{ cm}^{-3}$ were subjected to neutron irradiation and were cut to form match-like samples oriented along a selected crystallographic direction; the ratio of the length to the transverse dimensions of such “matches” was at least 10. The ends of the samples were ground, using a template, into regular tetrahedral pyramids; these ends were placed inside conical recesses 0.3–0.5 mm in diameter. The recesses were formed at the centers of brass pistons to which a deforming stress was applied. This avoided shear in the central part of the sample. The deformation homogeneity was monitored on the basis of broadening of the α_1 line which had no fine structure. Such broadening was practically undetectable (less than 5–10 μeV) right up to pressures of 500 kgf/cm^2 and remained slight at pressures of about 2000 kgf/cm^2 (less than 50 μeV).

Figure 2 shows the spectrum of the α_2 line obtained when a crystal was compressed along the [001] axis¹¹ and the evolution of the spectrum in a magnetic field applied along the same axis. The experimental and calculated, in accordance with Eq. (9), dependences of the spectral positions of the main Zeeman components on the magnetic field intensity H are plotted in Fig. 3. Figure 4 shows a scheme of radiative transitions from the state P_2 to the state P_1^* . The scheme is plotted on the basis of the expressions in Eq. (9). The values of the constants $\Delta_{\parallel} = -34.5$ and $\Delta_{\perp} = 38 \mu\text{eV}$ were selected to ensure an optimal agreement with the experimental

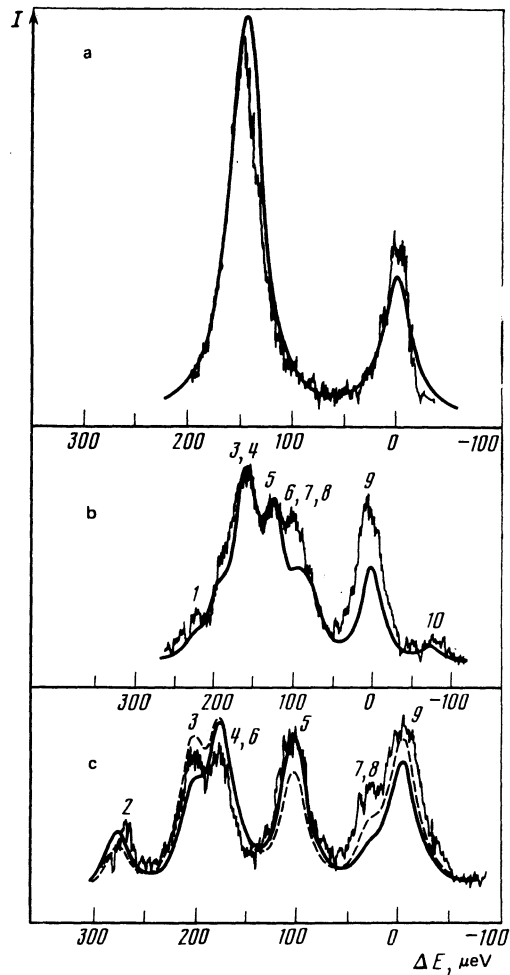


FIG. 2. Experimental and calculated spectra of the α_2 line at 2°K for silicon compressed along the [001] axis by a pressure $P \approx 400 \text{ kgf/cm}^2$ in the following magnetic fields: a) $H = 0$; b) 6 kOe; c) 15 kOe. The continuous curves represent calculations in the case of thermal-equilibrium populations of the spin sublevels; the dashed curve represents calculations for the ratio of the populations amounting to $S = 1$.

data. It was assumed that the g factors of electrons were the same and equal to the electron g factor in the case of a neutral donor, whereas the g factors of holes were taken to be the g

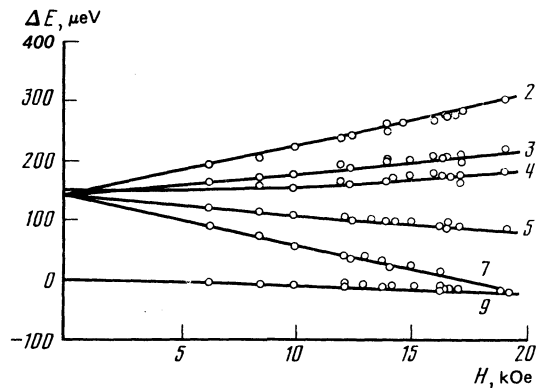


FIG. 3. Dependences of the spectral positions of the Zeeman components of the α_2 line at 2°K on the magnetic field $H \parallel [001]$ in the case of compression of silicon along the [001] axis by a pressure of $P \approx 400 \text{ kgf/cm}^2$. The continuous lines represent calculations based on Eq. (9).

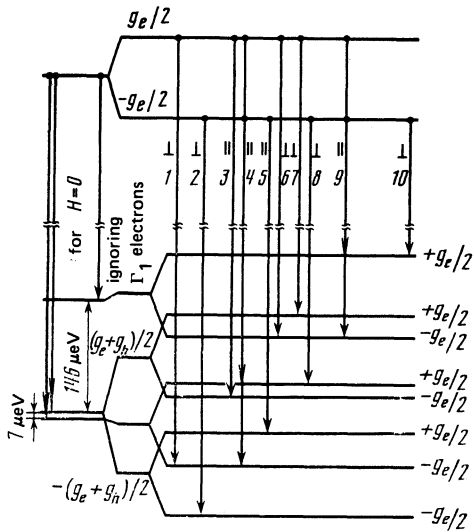


FIG. 4. Transition scheme for radiative dissociation of a complex P_2 accompanied by the creation of a complex P^* in an excited state when a magnetic field is applied to silicon subjected to pressure along the [001] axis.

factors of the ground state of a bound exciton.¹³ In a magnetic field the initial state P_2 split into two spin sublevels with $\pm 1/2\mu_0 g^e H$ because of the different orientations of the spin of the outer electron. In view of the equality of the electron g factors, the same splitting was obtained for the levels of the final state P^* because of the different orientations of the spin of the Γ_1 electron. Had the g factors of the electrons in the outer and inner shells been different, doubling of the components 4 and 9 in the Zeeman spectrum would have been observed. The allowed transitions were those without a change in projection of the momentum along the magnetic field direction (denoted by \parallel) and with a change in the projection of the momentum along ± 1 (denoted by \perp). It is clear from Fig. 3 that the spectral positions of the Zeeman components of the α_2 line are in good agreement with the calculations. In these calculations an allowance is made for the diamagnetic shift $\Delta E = bH^2$ with $b = 1.6 \times 10^{-2} \mu\text{eV}/\text{kOe}^2$ (Ref. 13), which is the same for all the components. One should also note the sublinear dependence of the shift of the components 4 and 9 on the magnetic field, which agrees with Eq. (9).

Figure 2 shows also the spectra calculated on a computer (continuous curves). The spectral positions of the peaks were calculated in accordance with Eq. (9) and with the transition scheme shown in Fig. 4; the peak profiles were set by the instrumental function of a Fabry-Perot interferometer¹⁸

$$I(\delta) = I_0 \left[1 + \left(\frac{2}{\pi} \mathcal{F} \sin \frac{\delta}{2} \right)^2 \right]^{-1}$$

TABLE I. Relative amplitudes of Zeeman components of α_2 line on compression along [001] axis.

Component	1	2	3	4	5	6	7	8	9	10
Amplitude	$\frac{a^2 s}{1+a^2}$	1	$4s$	$\frac{4(a^2 s + 1)}{1+a^2}$	$\frac{4}{1+a^2}$	$\frac{s}{1+a^2}$	s	$\frac{1}{1+a^2}$	$\frac{4(a^2 + s)}{1+a^2}$	$\frac{a^2}{1+a^2}$

with a finesse \mathcal{F} corresponding to the half-width of the α_1 line recorded under the same conditions (here δ is the phase shift acquired in the course of two trips through the interferometer). In calculating the amplitude relationships we assumed that the outer Γ_2 electron, which did not participate in the recombination process, retained its state during a radiative transition and that the probability of such a transition was determined completely by the state of an electron and a hole participating in the recombination process.¹³ We also assumed that the ratio of the populations of the upper and lower spin sublevels of the initial state corresponded to a thermal equilibrium and was $s = \exp(-g_e \mu_0 H / kT)$. The calculated amplitudes of the Zeeman components are listed in Table I, where the following notation is employed:

$$a^{-1} = \frac{h}{2\Delta_{\perp}} + \frac{|\Delta_{\perp}|}{\Delta_{\perp}} \left[1 + \left(\frac{h}{2\Delta_{\perp}} \right)^2 \right]^{1/2},$$

$$h = \frac{1}{2} \mu_0 (g^e - g^h) H, \quad s = \exp \left(-\frac{\mu_0 g^e H}{kT} \right).$$

The polarization introduced by the apparatus was allowed for by assuming that the ratio of the intensities of the transitions with the longitudinal and transverse polarizations was the same as for the corresponding Zeeman components of the α_1 line recorded under the same conditions.

It is clear from Fig. 2 that there was some discrepancy between the amplitude ratios in the experimental and calculated spectra. In the case of stronger magnetic fields ($H = 15$ kOe) the agreement could be improved by assuming that the populations of the spin sublevels of the initial P_2 state differed from equilibrium because of the long spin-lattice relaxation time of both free and bound charge carriers. The dashed curves in Fig. 2 represent the spectrum calculated on the assumption that the populations of the spin sublevels of the initial state ($s = 1$) are identical. The agreement could also be improved by allowing for the possibility of transitions accompanied by flipping of the spin of the Γ_2 electron. Since g_e was assumed to be the same for electrons in any state, this did not give rise to any new lines in the spectrum but simply altered the amplitude ratio.

The spectrum of the α_2 line obtained by applying tension to silicon in the direction of the [001] axis is plotted in Fig. 5. In agreement with Eq. (12), the final state P^* was found to split into four nondegenerate levels. An optimal agreement between the experiment and calculation (continuous curve in Fig. 5) was obtained for $A'_{\parallel} = 37 \mu\text{eV}$, $\Delta'_{\perp} = 1 \mu\text{eV}$, and $\Delta_T = 5 \mu\text{eV}$. The amplitudes of all four components were assumed to be the same. The agreement between the calculated and experimental spectra was satisfactory but it

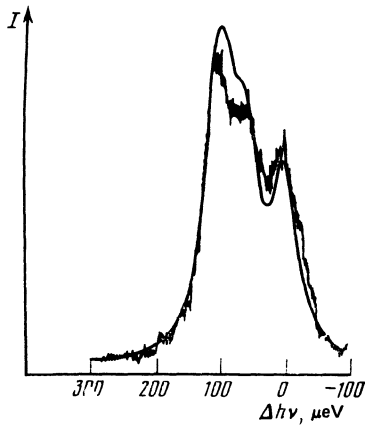


FIG. 5. Spectrum of the α_2 line at 2 °K for silicon stretched along the [001] axis by a force $P \approx -400$ kgf/cm². The continuous curve is calculated.

could probably be improved if allowance was made for transitions accompanied by flipping of the spin of the outer-shell electron.

We thus found that an allowance for the interaction of a hole with an outer-shell electron in an excited state P_1^* of a bound exciton makes it possible to provide a satisfactory quantitative description of the spectrum of the α_2 line obtained under uniaxial deformation of silicon along the [001] axis and of the evolution of this spectrum in a magnetic field. It should be stressed that had the splitting P_1^* been due to the interaction of a hole with an electron in the Γ_1 shell or due to the interaction of two electrons, the number, sequential order, and dependence of the shift of the Zeeman components on the magnetic field would have differed from those observed experimentally. Naturally, the interaction with the Γ_1 electron could give rise to an additional splitting of the terms, but within the limits of the resolution of our apparatus such splitting was not observed. This confirmed the initial assumption of our model that the interaction of a hole with an outer-shell electron has the dominant influence on the fine structure of the α_2 line.

4. FINE STRUCTURE OF THE α_2 LINE IN THE CASE OF UNIAXIAL DEFORMATION OF SILICON IN THE [111] AND [110] DIRECTIONS

As shown above, an analysis of the spectra of the α_2 line in the case when silicon was deformed along the simplest direction [001] made it possible to determine five constants linked to the interaction constants in the Hamiltonian (3) by the relationships (7) and (12). The constant Δ_0 describes the shift of the terms of the P_1^* state as a whole and does not affect the fine structure of the α_2 line. The constant Δ_6 represents the crystal splitting, which does not appear in our approximation if the uniaxial deformation along the [001], [111], or [110] axes is sufficiently strong. Hence, it follows that the splitting of the P_1^* level in the case when silicon is deformed along the [111] and [110] directions is governed by the eigenvalues of the Hamiltonian (3), (4) when the interaction constants have the values found in Sec. 3 for the [001] direction. The results of a numerical solution for the [111] and [110] directions of compression ($P > 0$) and tension

TABLE II. Splitting of P_1^* state for following interaction constants (μeV): $\Delta_1 = -3$, $\Delta_2 = 7$, $\Delta_3 = 109$, $\Delta_4 = -31$, $\Delta_5 = -18$, $\Delta_6 = 0$.

Stress	$P_{111} > 0$	$P_{111} < 0$	$P_{110} > 0$	$P = 0$	
Splitting	0	0	0	0	-154
	-64	-53	-63	-76	-160
	-91	-95	-102	-76	-160
	-119	-114	-119	-99	-163

($P < 0$), together with the constants Δ_1 - Δ_5 , are given in Table II. For convenience, Table I gives the energies of the levels P_1^* calculated from the energy level of the longest-wavelength component in the spectrum of the α_2 line.

Figures 6-8 show the spectra of the α_2 line which were obtained on compression and tension along the [111] axis and on compression along [110]. The spectra calculated on the basis of data on Table II are represented by continuous curves in these figures. The figures demonstrate a satisfactory agreement between the calculations and experiments. However, the discrepancies are somewhat greater than in the case of deformation along the [001] axis, and this applies also to the spectral positions of the components. However, we must bear in mind that in this comparison with the calculations we did not use any fitting parameters, because they were already determined in Sec. 3. Moreover, some of the constants (for example Δ_7) were obtained from Fig. 5 with a relatively low accuracy and this could have given rise to significant errors in the calculation of the interaction constants Δ_1 - Δ_5 . Moreover, our calculation was carried out in the approximation of an infinitely strong deformation, whereas in the experiments the splitting of the valence band could have been much greater than kT, but it amounted to just about 1 meV, i.e., it was not very large. As before, the discrepancy between the amplitudes can be attributed to the neglect of transitions accompanied by flipping of the spin of the outer electron.

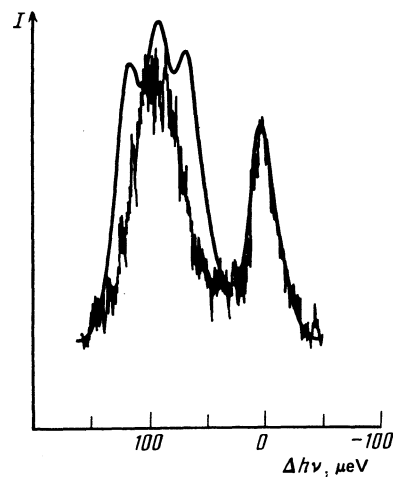


FIG. 6. Spectrum of the α_2 line at 2 °K for silicon compressed along the [111] axis by a pressure of $P \approx 400$ kgf/cm². The continuous curve is calculated.

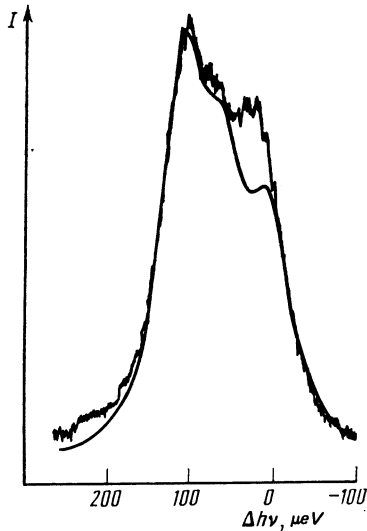


FIG. 7. Spectrum of the α_2 line at 2 °K for silicon stretched along the [111] axis by a force $P \approx -300$ kgf/cm². The continuous curve is calculated.

5. SPECTRUM OF THE α_2 LINE IN THE CASE OF UNDEFORMED SILICON

In this case the situation is most complex because the initial P_2 and final P_1^* states are split.

It is in principle possible to obtain the spectrum of the P_1^* state from an analysis of the fine structure of the γ_1 line, which appears on recombination of a bound exciton from an excited state, when one of its electrons is in the Γ_5 state, and the final state is an excited donor P_0^* in the same state. The lines γ_1 and γ_1^* were observed only in the experiments reported in Refs. 19 and 20 at temperatures 15–20 °K in the form of relatively weak singularities in the short-wavelength tail of the TA component of the free-exciton luminescence FE . Therefore, we attempted to obtain clearer γ_1 and γ_1^* lines by hf heating of an electron gas in order to excite a bound exciton to the P_1^* state. A sample was placed at a voltage antinode at the end of an open-circuited coaxial cable tuned to the resonance frequency of an external oscillator, and it was immersed in a helium bath. Figure 9 shows part of the luminescence spectrum of MEICs recorded without the use of an interferometer. It is clear from this figure that hf heating reduced very effectively the intensity of the α_m lines and made it possible to observe quite clearly the γ_1 and γ_1^* lines.

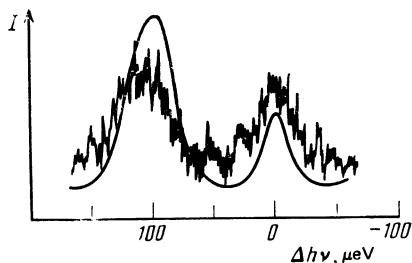


FIG. 8. Spectrum of the α_2 line at 2 °K for silicon compressed along the [110] axis by a pressure of $P \approx 300$ kgf/cm². The continuous curve is calculated.

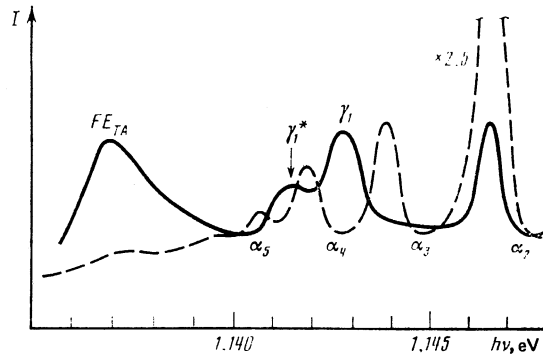


FIG. 9. Part of the luminescence spectrum of MEICs in silicon doped with phosphorus in a concentration of 6×10^{15} cm⁻³, recorded at 4.2 °K: the continuous curve was obtained in the presence of hf heating (at a frequency of 70 MHz); the dashed curve was recorded when the hf oscillator was switched off.

However, an interferometer analysis of the γ_1 line obtained in the hf heating case failed to reveal any distinguishable structure. It was likely that the hf heating broadened the components of the spectrum. Therefore, we simply calculated the final state. The splitting of the final state P_1^* was assumed to be governed by the eigenvalues of the Hamiltonian (3) where, in addition to the interaction constants Δ_1 – Δ_5 found in Sec. 3, there was an unknown constant Δ_6 representing the crystal splitting. In the calculations it was assumed that Δ_6 vanished. The results of this calculation are given in Table II.

In calculating the splitting of the initial state P_2 one should allow for the interaction of two holes in the Γ_8 shell and of an electron in the Γ_5 shell. The interaction of holes gives rise to the splitting $\{\Gamma_8 \times \Gamma_8\} = \Gamma_1 + \Gamma_3 + \Gamma_5$ (Ref. 3). If the outershell electron is considered as a spinor Γ_6 (Ref. 12), an allowance for the interaction with this electron gives rise to splitting into four levels: $\{\Gamma_8 \times \Gamma_8\} \times \Gamma_6 = \Gamma_7 + 2\Gamma_8$. An allowance for the real symmetry of an outer Γ_5 electron can generally give rise to splitting of the P_2 state into twelve levels: $\{\Gamma_8 \times \Gamma_8\} \times \Gamma_5 \times \Gamma_6 = 3\Gamma_6 + 3\Gamma_7 + 6\Gamma_8$. However, we can show that if only the pair interactions are allowed for and the intervalley matrix elements are ignored, the state P_2 splits into no more than six levels. An estimate of the splitting caused by the electron–hole interaction, obtained using the values of the constants Δ_1 – Δ_5 found in Sec. 3, shows that the splitting is of the order of 100 μ eV, i.e., it is of the same order of magnitude as the splitting of an exciton bound to a boron atom and is due to the interaction of holes. Therefore, the contribution of each of the interactions may be comparable. In view of the arbitrary nature of the selection of the interaction constants, we did not calculate the splitting of the initial state P_2 . As in Ref. 12, we felt able to postulate that the P_2 state splits into four groups of levels and we selected the separation between them so as to achieve the best agreement with the experimental results. Figure 10 shows the spectrum of the α_2 line in the absence of deformation, the energy level scheme of the final state P_1^* plotted in accordance with Table II, as well as the possible energy level scheme of the initial state P_2 . It is clear from this figure that the proposed scheme explains satisfactorily the energy posi-

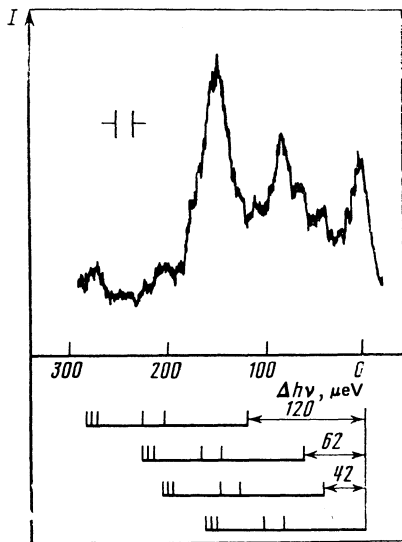


FIG. 10. Spectrum of the α_2 line obtained at 2 °K for $P = 0$. Under the spectrum the same energy scale is used to show by vertical marks (on four horizontal lines) the splitting of the final state P^* in accordance with Table II. The postulated splitting of the initial state P_2 , selected to ensure the best agreement between the calculated positions of the spectral components and the experimental results, corresponds to the shift of the scale of the P^* levels shown in the figure.

tions of the main components in the experimentally determined spectrum.

6. SPECTRA OF THE α_3 AND α_4 LINES

Figures 11 and 12 show the spectra of the α_3 and α_4 lines obtained for undeformed silicon, as well as the spectra of lines α'_4 and α''_4 corresponding to the recombination of a hole from the states $3/2$ and $1/2$, respectively, when silicon was subjected to a uniaxial compression along the $[111]$ axis. It is clear from these figures that the fine structure details did not appear in these spectra although the resolution of the apparatus was sufficiently high. This could be due to a large number of components in the luminescence spectrum, because in the initial and final states there were several particles and the interaction between them could give rise to splitting. Moreover, as pointed out in Ref. 12, in the final excited state P_{m-1}^* the number of electrons in the outer shell is $m - 1$.

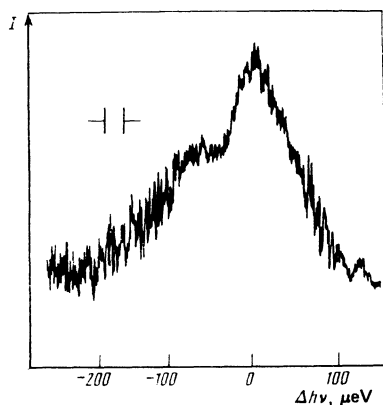


FIG. 11. Spectrum of the α_3 line at 4.2 °K for $P = 0$.

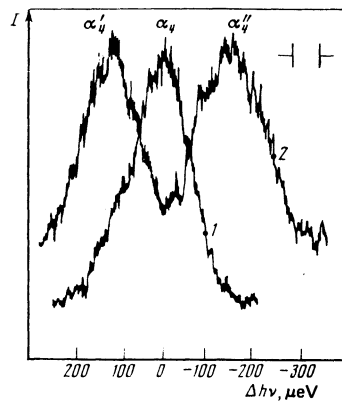


FIG. 12. Spectrum of the α_4 line at 4.2 °K: 1) $P = 0$; 2) $P = 80$ kgf/cm² along the $[111]$ axis.

The probability of transitions of these electrons to the ground state should increase and the lifetime of an excited state should decrease as m is increased. The reduction in the lifetime may give rise to broadening of the final-state levels and to overlap of the spectral components. However, one should draw attention to very different profiles of the components α'_4 and α''_4 (Fig. 12). These lines are emitted under conditions when the electron configurations of the initial and final states are equivalent, and the difference between them occurs only in the hole states. This difference provides one more confirmation of the justification for our initial assumption that there is need to allow for the electron-hole interaction.

7. CONCLUSIONS

Experimental and theoretical investigations of the fine structure of no-phonon lines in the luminescence due to MEICs bound to donors in silicon made it possible to draw a number of conclusions about the nature of the interaction of electrons and holes in such complexes. Above all, it should be stressed that the interaction with electrons in the inner shell Γ_1 does not cause splitting of the levels in the initial and final states. Therefore, the interaction with the Γ_1 electrons can be ignored in the calculation of the energy spectrum of MEICs. We shall assume that an MEIC in the ground and excited states can be regarded, respectively, as a system comprising a center with a negatively charged or a neutral donor and a system of the remaining electrons and holes which do not perturb greatly this center. The validity of such an approximation can simplify greatly the construction of a quantitative model. A comparison of the experimental and calculated results made in the present paper has enabled us to estimate directly the constants of the electron-hole exchange interaction. We are of the opinion that the values of these constants can be used in discussing other many-particle complexes. The results show that the shell model^{2,3} needs correction in developing a quantitative theory of MEICs.

The authors are grateful to G. E. Pikus for a valuable discussion of the results.

¹⁾ In Ref. 12 we reproduced the spectrum of the α_4 line in the case of insufficiently strong compression along the $[001]$ axis, which gave rise to an "excess" component 2, corresponding to a transition from the excited state P_2 .

- ¹A. S. Kaminskiĭ and Ya. E. Pokrovskii, *Pis'ma Zh. Eksp. Teor. Fiz.* **11**, 381 (1970) [*JETP Lett.* **11**, 255 (1970)].
- ²G. Kirczenow, *Solid State Commun.* **21**, 713 (1977).
- ³G. Kirczenow, *Can. J. Phys.* **55**, 1787 (1977).
- ⁴A. S. Kaminskiĭ and Ya. E. Pokrovskii, *Problemy sovremennoĭ radio-tekhniki i elektroniki (Problems in Modern Radio Engineering and Electronics)*, Nauka, M., 1980, p. 455.
- ⁵V. D. Kulakovskii, G. E. Pikus, and V. B. Timofeev, *Usp. Fiz. Nauk* **135**, 237 (1981) [*Sov. Phys. Usp.* **24**, 815 (1981)].
- ⁶A. S. Kaminskiĭ and Ya. E. Pokrovskii, *Zh. Eksp. Teor. Fiz.* **75**, 1037 (1978) [*Sov. Phys. JETP* **48**, 523 (1978)].
- ⁷G. L. Bir and G. E. Pikus, *Simmetriya i deformatsionnye éffekty v poluprovodnikakh*, Nauka, M., 1972 (*Symmetry and Strain-Induced Effects in Semiconductors*, Wiley, N. Y., 1975).
- ⁸R. L. Aggarwal and A. K. Ramdas, *Phys. Rev.* **137**, A602 (1965).
- ⁹W. E. Krag, W. H. Kleiner, and H. J. Zeiger, *Proc. Tenth Intern. Conf. on Physics of Semiconductors*, Cambridge, Mass., 1970, publ. by US Atomic Energy Commission, Washington, D. C. (1970), p. 271.
- ¹⁰A. Natori and H. Kamimura, *J. Phys. Soc. Jpn.* **43**, 1270 (1977).
- ¹¹R. R. Parsons, *Solid State Commun.* **22**, 671 (1977).
- ¹²A. S. Kaminskiĭ, V. A. Karasyuk, and Ya. E. Pokrovskii, *Pis'ma Zh. Eksp. Teor. Fiz.* **33**, 141 (1981) [*JETP Lett.* **33**, 132 (1981)].
- ¹³A. S. Kaminskiĭ, V. A. Karasyuk, and Ya. E. Pokrovskii, *Zh. Eksp. Teor. Fiz.* **79**, 422 (1980) [*Sov. Phys. JETP* **52**, 211 (1980)].
- ¹⁴G. E. Pikus, *Zh. Eksp. Teor. Fiz.* **41**, 1258 (1961) [*Sov. Phys. JETP* **14**, 898 (1962)].
- ¹⁵A. S. Kaminskiĭ, V. A. Karasyuk, and Ya. E. Pokrovskii, *Zh. Eksp. Teor. Fiz.* **74**, 2234 (1978) [*Sov. Phys. JETP* **47**, 1162 (1978)].
- ¹⁶G. L. Bir, G. E. Pikus, L. G. Suslina, and D. L. Fedorov, *Fiz. Tverd. Tela (Leningrad)* **12**, 1187 (1970) [*Sov. Phys. Solid State* **12**, 926 (1970)].
- ¹⁷G. E. Pikus and N. S. Averkiev, *Pis'ma Zh. Eksp. Teor. Fiz.* **34**, 28 (1981) [*JETP Lett.* **34**, 26 (1981)].
- ¹⁸M. Born and E. Wolf, *Principles of Optics*, 4th ed., Pergamon Press, Oxford, 1970 (Russ. Transl., Nauka, M., 1973).
- ¹⁹M. L. W. Thewalt, *Can. J. Phys.* **55**, 1463 (1977).
- ²⁰E. C. Lightowers, M. O. Henry, and M. A. Vouk, *J. Phys. C* **10**, L713 (1977).

Translated by A. Tybulewicz